Available online at www.sciencedirect.com

ScienceDirect

JOURNAL OF IRON AND STEEL RESEARCH, INTERNATIONAL. 2015, 22(11): 1055-1061

Effect of Chromium on Microstructure and Mechanical Properties of Cold Rolled Hot-dip Galvanizing DP450 Steel

Yun HAN, Shuang KUANG, Hua-sai LIU, Ying-hua JIANG, Guang-hui LIU
(Shougang Research Institute of Technology, Beijing 100043, China)

Abstract: Two cold rolled hot-dip galvanizing dual phase (DP) 450 steels with different amounts of chromium were designed and the effects of the chromium concentration and galvanizing processes on the microstructure and mechanical properties were also investigated. The results show that the experimental steels exhibit typical dual phase microstructure character. However, the ferrite phase of steel with higher chromium is more regular and its boundaries are clearer. Meanwhile, martensite austenite (MA) island in steel No. 2 is diffused and no longer distributes along the grain boundary as net or chain shape. More MA islands enriched with Cr element can be found in the ferrite grains, and the increment of Cr element improves the stablity of the austenite so that the austenite has been reserved in MA islands. In addition, the experimental steel with higher chromium exhibits better elongation, lower yield ratio and better formability. The mean hole expanding ratio of steels No. 1 and No. 2 is 161.70% and 192.70%, respectively.

Key words: DP steel; high chromium; microstructure; mechanical property; formability

The energy conservation, emissions reduction and safety of the car body have become the development trend of the automotive industry. Because of the low yield strength, high beginning hardening rate, high strength, good plasticity, high impact energy absorption and good bent resistance, the cold rolled dual phase (DP) steel shows great superiority and good prospects in the vehicle mass reduction[1-10]. Moreover, low grade cold rolled DP steels, which have excellent combined mechanical properties, can be used in both automotive structural parts and covering parts.

In the cold rolled hot-dip galvanizing DP steel, large amount of alloying elements should be added to enhance the hardenability so that martensite can be formed during cooling after the galvanizing. However, excess Si and Mn elements usually enrich on the surface of the steel, which is harmful to the galvanizing quality. Thereby, some Cr and Mo elements should be added to partly replace Si and Mn[11-13]. However, the addition of alloying elements might induce some effects on the mechanical properties of the steel by affecting the alloy distribution in both martensite and ferrite and futher affects its formability[14].

In this work, two cold rolled hot-dip galvanizing DP450 steels with different chromium concentrations were designed and the effects of the chromium concentration and galvanizing on the microstructure and mechanical properties were also investigated.

1 Experimental

The chemical compositions of the experimental steels are listed in Table 1. It can be seen that steel No.2 has lower carbon and higher chromium compared with steel No.1.

The experimental steel was fabricated by 50 kg vacuum induction furnace and cast into square ingots. The ingots were homogenized at 1 200 °C for 1 h and then rolled to 4 mm plate. The finished rolling temperature and simulating coiling temperature were 870 °C and 660 °C, respectively. The plates were then air cooled to room temperature. After hot rolling, the plates were cold rolled to 1.5 mm in thickness. The galvanizing cycle in Fig. 1 was simulated by a multi-purpose simulator in laboratory and the galvanizing cycle parameters are listed in Table 2.

The tensile samples were cut from the experimental steels and the tensile test was conducted on a universal materials tester at room temperature. The specimens were prepared by polishing and etching in nital or Lepera

Table 1 Chemical compositions of designed steel mass%

Steel	C	Si	Mn	Cr	Al	P	S
No. 1	0.08	0.08	1.30	0.20	0.05	<0.02	<0.007
No. 2	0.06	0.09	1.25	0.50	0.05	<0.02	<0.007

Biography: Yun HAN, Doctor, Engineer; **E-mail:** hanyun@shougang.com.cn; **Received Date:** August 12, 2014

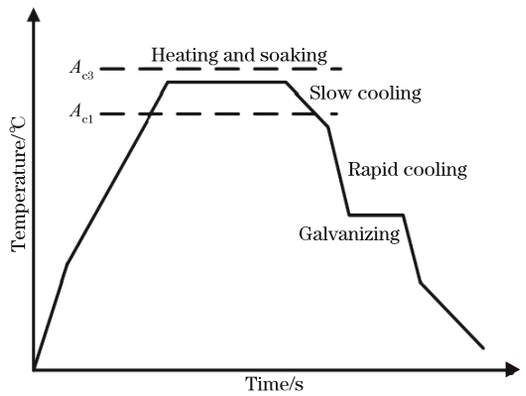

Fig. 1 Diagrammatic sketch of the galvanizing cycle

solution to observe their microstructures and martensite austenite (MA) islands by optical microscopy (OM), scanning electron microscopy (SEM), energy dispersive X-ray spectroscopy (EDS) and transmission electron microscopy (TEM).

2 Results and Discussion

2.1 Mechanical properties of experimental steels

Fig. 2 shows the mechanical properties of the experimental steels experienced various galvanizing simulation. It was known from Table 2 that the difference of the galvanizing parameter concentrates on the heating temperature, soaking temperature and slow cooling temperature. Generally speaking, as the temperature increases,

Table 2 Parameters of galvanizing cycle ℃

Process No.	Preheating temperature	Heating temperature	Soaking temperature	Slow cooling temperature	Galvanizing temperature
1	220	760	760	680	460
2	220	780	780	690	460
3	220	800	800	700	460

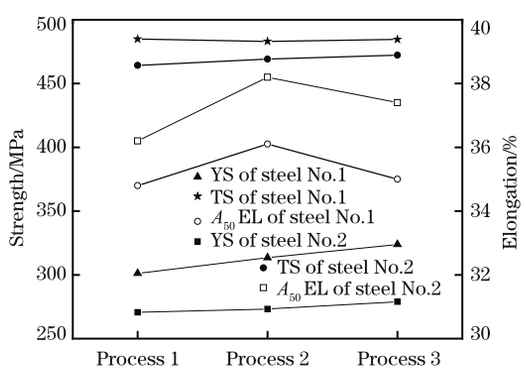

Fig. 2 Mechanical properties of the experimental steels through various processes

both tensile strength (TS) and yield strength (YS) are enhanced slightly. This phenomenon may be attributed to the increment of austenite fraction which could be transformed into martensite during the following cooling. Nevertheless, the elongation (EL) variation is not monotonic. Both steels No. 1 and No. 2 experienced process 2 and have the best elongation. Furthermore, it is worth noticing that steel No. 2 has lower strength and higher elongation for any process compared with steel No. 1. However, the decrement of yield strength of steel No. 2 is more obvious. From Fig. 2, the best combined mechanical properties of steels No. 1 and No. 2 can be concluded as 483.1 MPa (TS), 313.5 MPa (YS), 36.1% (A_{50} EL) and 469.1 MPa (TS), 273.2 MPa (YS), 38.2% (A_{50} EL) respectively, all of which are satisfied to the mechanical properties of DP450 steel. However, the steel No. 2 exhibits much better elongation and lower yield ratio, indicating the better forming ability of such steel.

2.2 Microstructure of experimental steels

The samples of experimental steels experienced many processes, which were etched by Lepera solution for microstructure observation, as shown in Fig. 3.

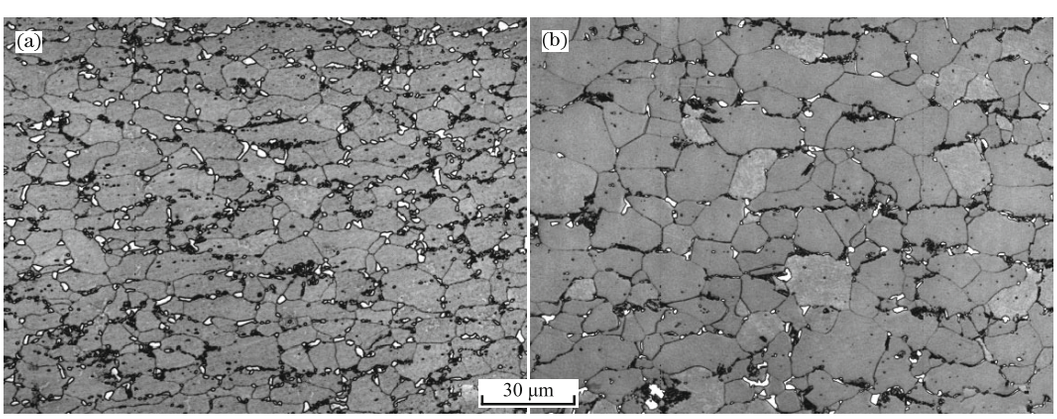

Fig. 3 Microstructure and MA island distribution of steels No. 1 (a) and No. 2 (b)

Figs. 3(a) and 3(b) show the microstructure and MA island distribution of steels No. 1 and No. 2, respectively. It can be seen that the experimental steels exhibit typical dual phase microstructure character which consists of grey polygonal ferrite, bright white MA island along with ferrite grain boundaries and little black bainite. It should be noted that the ferrite of steel No. 2 (Fig. 3(b)) is more regular and its boundaries are clearer than that of steel No. 1 (Fig. 3(a)). Meanwhile, the amount of the bainite and MA island in steel No. 2 is also less than that of steel No. 1. The volume fraction of MA island in steels No. 1 and No. 2 is 1.26% and 0.98%, respectively. Moreover, the MA island in steel No. 2 is diffused and no longer distributes along the grain boundary as net or chain shape.

Fig. 4 shows the MA island distribution of the steels were examined by SEM through process 2. It is clear that the MA islands in steel No. 1 (Fig. 4(a)) mainly distributes along the grain boundaries. However, for steel No. 2, a large amount of MA islands are located inside the grains (Fig. 4(b)).

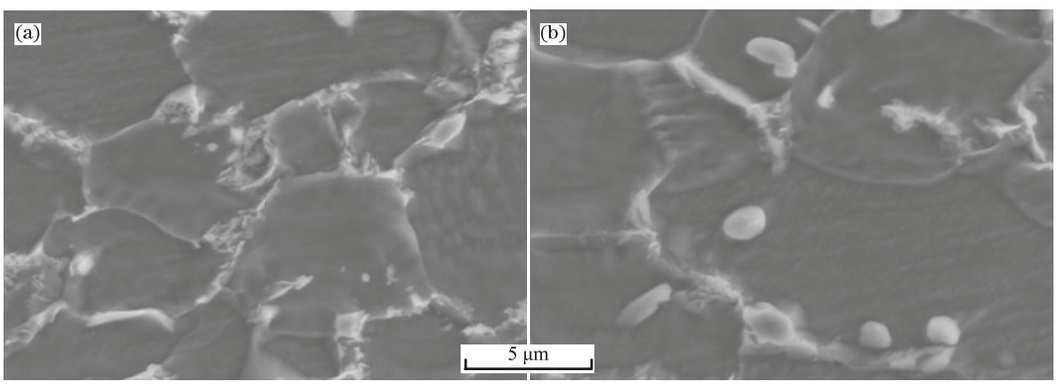

Fig. 4 MA island distribution of experimental steels No. 1 (a) and No. 2 (b) examined by SEM

2.3 EDS analysis of experimental steels

In order to identify the difference of the MA islands located in different positions, the energy dispersive X-ray spectroscopy (EDS) analysis was performed. Spectrums of differfent MA islands are plotted in Fig. 5. It can be seen that spectrums 1, 2 and 4 are MA island inside the grain, and spectrum 3 is MA island along the grian boundary. In addition, spectrums 5 which represents the matrix is also examined and compared with other results.

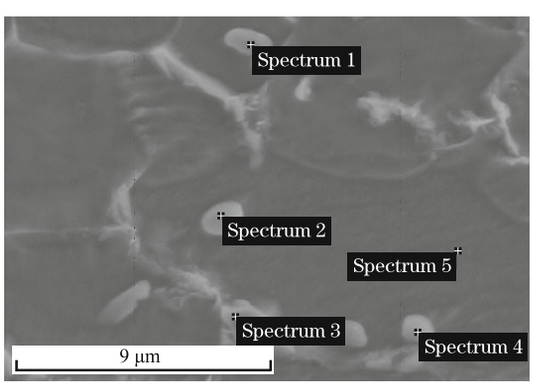

Fig. 5 EDS analysis of the MA islands

The composition analysis results are listed in Table 3. It can be seen that the MA islands inside ferrite grain (spectrums 1, 2 and 4) contain higher Cr and Mn elements but relatively lower C element. As for the MA island along the grain boundary (spectrum 3), C element is enriched while Cr and Mn elements are depleted. For the ferrite matrix, the result of spectrum 5 shows that it contains the lowest amount of C, Mn and Cr. Moreover, it is worth noticing that the amount of both Cr elements and Mn elements in MA island along the grain boundary is nearly the same as that in ferrite matrix. Thus, it can be concluded that MA islands along the grain boundary are formed depending on the enrichment of C elements. Nevertheless, the Cr and Mn tend to enrich in the grain and form the MA island in the grain accordingly. This implies that higher Cr addition can promote the increase of MA islands in the ferrite grain. Meanwhile, the amount of MA islands which are enriched with C and distributed along the grain boundary will decrease.

Table 3 Composition analysis results of MA islands by EDS

mass%

Spectrum	C	Cr	Mn	Fe	Total
Spectrum 1	9.71	1.31	3.55	85.43	100.00
Spectrum 2	11.29	1.77	3.74	83.20	100.00
Spectrum 3	12.47	0.62	1.05	85.86	100.00
Spectrum 4	8.99	1.06	2.07	87.88	100.00
Spectrum 5	7.44	0.53	1.04	91.00	100.00

2.4 TEM analysis

Except the amount of MA islands, the morphology of them is also important for the mechanical properties of DP steel. Fig. 6 shows the results of TEM analysis of the experimental steels. Figs. 6(a)-6(d) show the microstructure

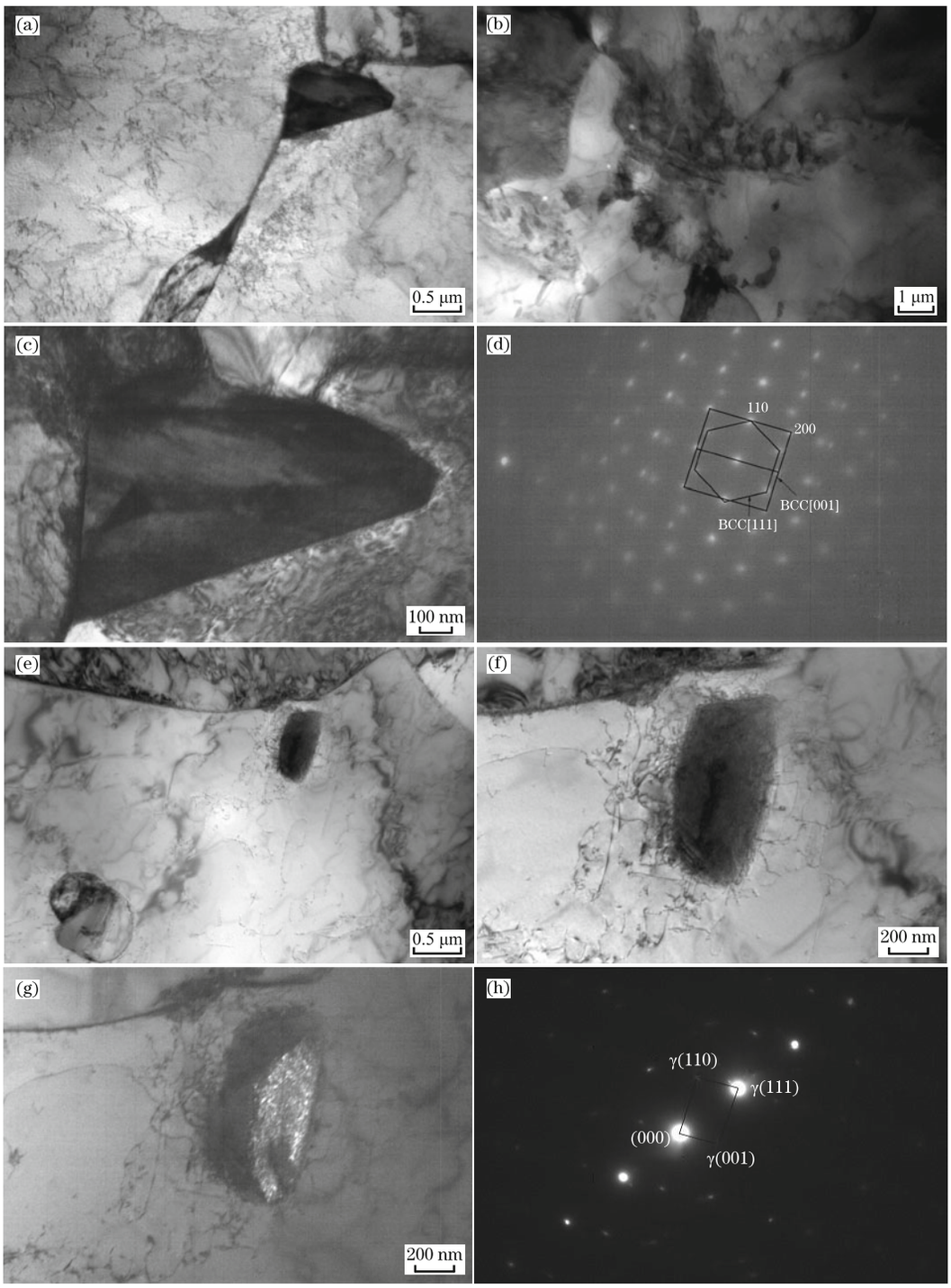

Fig. 6 TEM analysis of steel No. 1 (a-d) and steel No. 2 (e-h)

and the selected area electron diffraction (SAED) of steel No. 1, while Figs. 6(e)-6(h) show that of steel No. 2. From Fig. 6(a), it is clear that MA islands with triangular shape distribute along the grain boundary, and lots of dislocations spread in the ferrite grain. Moreover, from Fig. 6(b), bainite microstructure can also be easily found in steel No. 1, which can enhance the strength of the steel. Figs. 6(c) and 6(d) show the magnified image of the typical MA island in steel No. 1 and its selected area electron diffraction pattern, respectively. It can be seen that MA island has different orientations which exhibit various diffraction patterns in Fig. 6(d). However, all of the diffraction patterns are typical BCC structure patterns which are marked in Fig. 6(d) as BCC [001] and BCC [111], respectively. As for steel No. 2, MA island distributed in the ferrite grain can be easily found, as shown in Fig. 6(e). Furthermore, the dislocation density in the ferrite grain of steel No. 2 seems lower than that in steel No. 1 (Fig. 6(a)). It may be attributed to the lower carbon content in the matrix which makes the ferrite

much cleaner. At last, it might play an important role in decreasing the yield ratio and improving the forming properties of the steel. Fig. 6(f) shows the magnified image of the typical MA island in the grain. It can be found that the dislocations pile up around MA island which implies the strengthening of the steel. In order to analyze the structure of the MA island, Figs. 6(g) and 6(h) show the dark field image of the selected area and its electron diffraction pattern. It shows that different structures can be observed and its electron diffraction pattern exhibits the FCC structure (Fig. 6(h)).

2.5 Formability of experimental steels

Hole expansion test is regarded as an effective method to evaluate the formability of steel. Hence, hole expansion tests were performed for the experimental steels and the results are shown in Fig. 7 and Table 4. Fig. 7 shows the images of hole expansion samples of experimental steels. Figs. 7(a)-7(c) show steel No. 1 while Figs. 7(d)-(f) shows steel No. 2. From Fig. 7, it can be observed obviously that the hole diameter of steel No. 2 after expansion is larger than that of steel No. 1. Furthermore, the detailed parameters of the results are given in Table 4. It is clear that steel No. 2 has larger hole diameter after cracking, which implies a better hole expanding ratio. The mean hole expanding ratio of steels No. 1 and No. 2 is 161.70% and 192.70%, respectively. Thus, steel No. 2 should have better formability in comparison with steel No. 1.

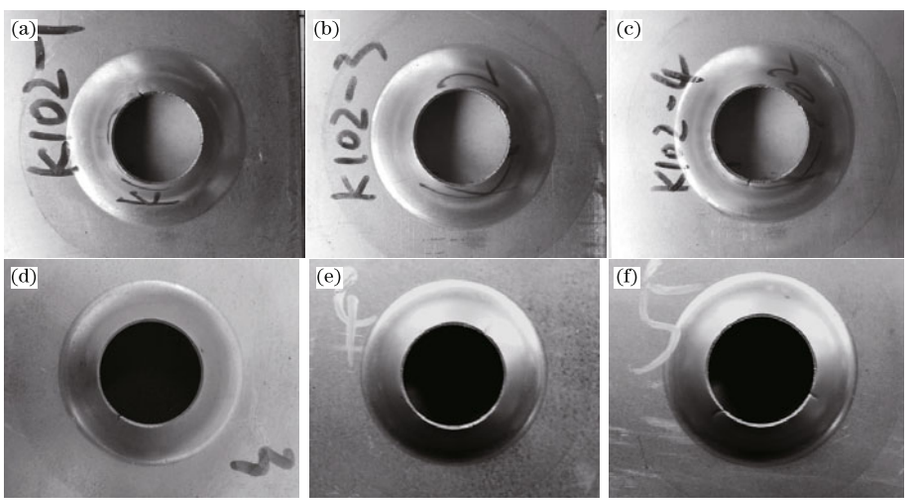

(a), (b), (c) Steel No.1; (d), (e), (f) Steel No.2.

Fig. 7 Images of hole expansion samples of experimental steels

Table 4 Hole expansion results of experimental steels

Steel	Initial hole diameter/mm	Hole diameter after cracking/mm			Hole expanding ratio/%	Mean hole expanding ratio/%
		D1	D2	Mean		
No.1	10.00	25.44	25.38	25.41	154.10	161.70
	10.00	26.24	26.15	26.20	161.95	
	10.00	26.94	26.87	26.91	169.05	
No.2	10.00	29.22	29.26	29.24	192.40	192.70
	10.00	29.20	29.33	29.27	192.70	
	10.00	29.25	29.35	29.30	193.00	

2.6 Thermodynamic analysis

In order to clarify the microstructure evolution, the Thermo-Calc software was used to calculate the phase mass fraction and the elements content in various phases. The calculated results are shown in Figs. 8 and 9, respectively. Fig. 8 shows the phase transformation and its mass fraction of the experimental steels. It can be seen that, at the same process temperature, the mass fraction of ferrite (BCC) of steel No. 2 is more than that of steel No. 1 while mass fraction of austenite (FCC) of steel No. 2 is less than that of steel No. 1. This may be attributed to the increase of the Cr element amount of steel No. 2 which is the typical ferrite former element. It means that the ferrite in the steel No. 2 is easier to be formed and the volume fraction will increase accordingly compared to steel No.1 at the same temperature. Hence, the amount of MA island in steel No. 1 will be more than that in steel No. 2 which is transformed from austenite during the cooling process. Thus, the microstruture results shown in Figs. 3 and 4 can be explained.

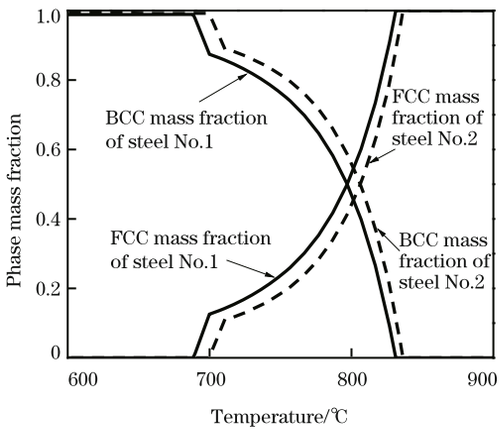

Fig. 8 Phase fraction of experimental steels calculated by Thermo-Calc

Furthermore, Fig. 9 shows the mass fraction of Cr and C elements in various phases. It can be seen from Fig. 9(a) that Cr element has obvious increase in both ferrite and austenite of steel No. 2. It is well known that Cr element can enhance the hardenability of the austenite. Thus, the amount of bainite will decrease during cooling which has been observed in Figs. 3 and 6. In addition, the increment of Cr element in austenite also improves the stablity of the austenite so that it cannot be transformed to martensite completely. The stable austenite has been reserved as shown in Figs. 6(g) and 6(h). It is clear that the MA island consists of partial martensite and partial austenite, which makes it not too hard so that the crack will not be formed easily along the phase boundary during the material forming process. Besides that, it is important that Cr element also has effects on improving the shape

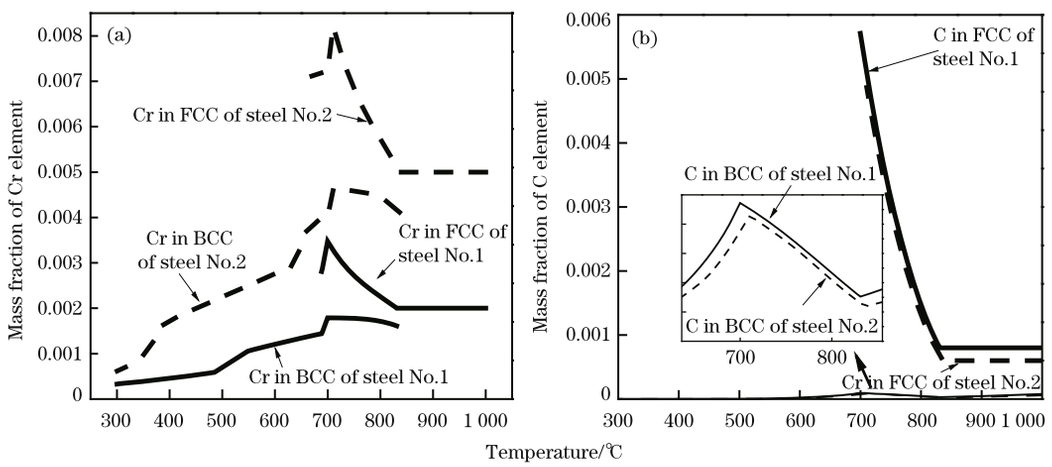

(a) Cr element; (b) C element.

Fig. 9 Mass fraction of the elements in various phases calculated by Thermo-Calc

and distribution of martensite. Just like the results shown in Fig. 5 and Table 3, higher Cr addition can promote the increase of MA islands in the ferrite grain. Meanwhile, the MA islands become diffusive and nearly spheric[12,13].

Fig. 9(b) shows the C element mass fraction of experimental steels in ferrite and austenite phases. It can be seen that the difference between steels No. 1 and No. 2 is not obvious because the amount of that is limited. However, the magnified curve of the C mass fraction in ferrite is exhibited in the figure, and the C mass fraction of steel No. 2 is still lower than that of steel No. 1. Moreover, considering the results shown in Fig. 8, the ferrite amout of steel No. 2 is more than that of steel No. 1 at the same temperature. It implies that the mean C mass fraction of steel No. 2 in ferrite is much lower than that of steel No. 1. Therefore, the decrease of C element makes the ferrite purer and its ductility is enhanced accordingly.

Above all, compared with steel No. 1, the microstructure of steel No. 2 mainly consists of large amount of purer polygonal ferrite with high ductility and some diffusive MA islands. This microstructure is helpful to decrease the yield strength and yield ratio of the experimental steel[15,16]. Moreover, the amount of MA islands in ferrite grain of steel No. 2 increases because of the Cr addition.These MA islands are rich in Cr elements and consist of some stable reserved austenite. During the forming process, the softer MA island is helpful to coordinate the deformation, so that the crack will not be formed along the phase boundaries easily. Meanwhile, more mobile dislocation will be produced in the ferrite around the deformed MA island which can further strengthen the steel.

3 Conclusions

(1) Experimental steel with lower carbon and higher chromium (steel No. 2) has better elongation and lower yield ratio. The combined mechanical properties are 469.1 MPa (TS), 273.2 MPa (YS), and 38.2% (A_{50} EL), respectively.

(2) Experimental steels exhibit typical dual phase microstructure character which consists of polygonal

ferrite, MA island and little bainite. However, ferrite of steel with lower carbon and higher chromium is more regular and its boundaries are clearer. Meanwhile, the amount of the bainite and MA island in it is also less.

(3) MA island in steel No. 2 is diffused and no longer distributes along the grain boundary as net or chain shape. More MA islands enriched with Cr elements can be found in the ferrite grain. Meanwhile, the increment of Cr element improves the stability of the austenite so that the stable austenite has been reserved in MA island.

(4) MA island with partial reserved austenite is helpful to coordinate the deformation, so that the steel No.2 has better formability compared with steel No. 1. The mean hole expanding ratio of steels No. 1 and No. 2 is 161.70% and 192.70%, respectively.

References:

[1] Y. L. Kang, Theory and Technology of Process and Formation for Advanced Automobile Steel Sheets, Metallurgical Industry Press, Beijing, 2009.

[2] K.S. Parka, K. Parkb, D. L. Lee, C. S. Lee, Mater. Sci. Eng. A 499-451 (2007) 1135-1138.

[3] M. H. Akbarpour, A. Ekrami, Mater. Sci. Eng. A 475 (2008) 293-298.

[4] X. Liang, J. Li, Y. H. Peng, Mater. Lett. 62 (2008) 327-329.

[5] S. Kuang, Y. L. Kang, H. Yu, R. Liu, Int. J. Miner. Metall. Mater. 16 (2009) 159-164.

[6] J. J. Luo, W. Shi, Q. F. Huang, L. Li, J. Iron Steel Res. Int. 17 (2010) No.1, 54-58.

[7] Q. H. Han, Y. L. Kang, X. M. Zhao, C. Lü, L. F. Gao, J. Iron Steel Res. Int. 18 (2011) No.5, 52-58.

[8] H. Fatih, U. Hüseyin, J. Iron Steel Res. Int. 18 (2011) No.8, 65-72.

[9] F. Ozturk, S. Toros, S. Kilic, J. Iron Steel Res. Int. 16 (2009) No.6, 41-46.

[10] A. Hüseyin , K.Z. Hawa, K. Ceylan, J. Iron Steel Res. Int. 17 (2010) No.4, 73-78.

[11] K. Hasegawa, K. Kawamura , T. Urabe, Y. Hosoya, ISIJ Int. 44 (2004) No.3, 603-609.

[12] H. Q. Han, Study of Microstructure and Property of Cold Rolled and Continuous Annealed DP Steel with Low C-Si-Mn System, Northeastern University, Shenyang, 2009.

[13] F. Niu, A. M. Zhao, Z. Z. Zhao, G. C. Jin, C. Tian, J. Iron Steel Res. 22 (2010) No.7, 47-50.

[14] G. Süleyman, Mater. Lett. 63 (2009) 2381-2383.

[15] J. Lis, A. K. Lis, C. Kolan, J. Mater. Process. Technol. 162-163 (2005) 350-354.

[16] M. Erdogan, S. Tekeli, Mater. Des. 23 (2002) 597-604.